International Journal of Advances in Engineering and Management (IJAEM)
Volume 3, Issue 6 June 2021, pp: 1139-1147 www.ijaem.net ISSN: 2395-5252

Comparative Study of Ducted and Unducted Propeller

[1]Mahankali Pradeep, [2]Sheikh Misbah Ul Haque, [3]k. Sai Priyanka
[1,2]*Under-Graduate Students, Aeronautical Engineering, Institute of Aeronautical Engineering, Dundigal, Hyderabad, Telangana.*
[3]*Assistanat Professor, Department of Aeronautical Engineering,Institute of Aeronautical Engineering, Dundigal, Hyderabad, Telangana.*

Submitted: 01-06-2021 Revised: 14-06-2021 Accepted: 16-06-2021

ABSTRACT: The purpose of the research is to evaluate the performance characteristics of a ducted propeller in comparison to an unducted propeller. The design requirements of a propeller are nowadays more demanding not only to provide high efficiency but to provide also low induced vibrations and low radiated noise. A ducted propeller may represent a possible solution to the problem even though its main application is devoted to have a highly efficient propeller. In this case, the duct we generated accelerates flow generated by the propeller, assisting a lift force pointing ahead, and thus increasing propeller thrust and we have done a comparative study of aerodynamic performance of a ducted propeller and non-ducted propeller having same design configurations. We have done preliminary analysis of propeller using Qblade software and further both the propellers were modelled in CATIA and analyzed in ANSYS fluent pressure based solver using transient simulation by sliding mesh approach model using k-epsilon turbulence model. The expected result is to have a better aerodynamic performance of the ducted propeller than its counterpart.

KEYWORDS:CFD, k-epsilon turbulence model, ducted propeller, thrust, aerodynamic performance, transient, pressure-based solver, sliding mesh approach, unducted propeller.

I. INTRODUCTION

A propeller could be thought of as a rotating wing that assembles aerofoils into a single unit, similar to the cross-section of an airplane's wing. A simple propeller configuration consists of at least two blades connected by a central hub. By translating the rotational force from the engine shaft into thrust, the aircraft is propelled forward through the air. The aerofoil's chamber design allows the airflow in front of the blade to fly at a faster rate. The movement of the airflow induces a decrease in static pressure in front of the blade, according to Bernoulli's theory. Meanwhile, the propeller is subjected to higher static pressure due to lower speed at the back of the propeller. As a result of the reaction force, the aircraft is forced forward as the pressure at the front decreases. The pressure differential between the front and back sections of the propeller generates thrust in forward directions, allowing the aerial vehicle to withstand drag. Unmanned Aerial Vehicles (UAVs) propellers have a small diameter, operate at a low Reynolds number, and have a low tip speed. Based on the chord at 75 percent span position, the Reynolds number considered in this study is less than 27000. The aim of this research is to look at one method for determining the efficiency of a propeller blade that is operating at a low Reynolds number. The aim of this research is to use CFD software (FLUENT) to simulate the flow of a propeller blade in order to determine the thrust coefficient, power coefficient, and performance.

PROPELLERTHEORY

They are two popular theories for propeller design
1) Momentum Theory.
2) Blade Element Theory.

MOMENTUM THEORY:

The propeller is modelled in momentum theory as a simple actuator disk that accelerates flow in the axial direction by generating a pressure jump in the propeller plane. AE/A0 = 1 when the propeller is seen as a continuous circular disk with infinite blades. The model is much too crude to be useful in propeller design, but it does provide some insight into a propeller's global mechanism.

$T = \rho.A.V.\ (Ve - V\infty)$

$A_0 = \pi D^2 /4.$

International Journal of Advances in Engineering and Management (IJAEM)
Volume 3, Issue 6 June 2021, pp: 1139-1147 www.ijaem.net ISSN: 2395-5252

The momentum theory considers the propeller plane's inflow and outflow to be the flow through a tube with a varying cross-section but always a circular form. The momentum theory considers the propeller plane's inflow and outflow to be the flow through a tube with a varying cross-section but always a circular form. The higher the efficiency, the smaller the rise in velocity caused by the propeller. If the downstream velocity is the same as the upstream velocity. One method of modelling this effect is to use blade element theory.

BLADE ELEMENT THEORY:

By splitting each blade into a number of parts, known as blade components, the blade element theory (BET) aims to estimate the thrust of a propeller. Each variable is treated as a separate two-dimensional entity in the theory. The aerodynamic forces can be determined based on the local flow conditions at the element using an airfoil. Then, after determining the aerodynamic properties, they are then added together to determine the properties of the whole propeller. Propellers typically have morphing airfoil forms, which evolve over time. From a thick airfoil at the hub to a thin one at the top, the airfoil changes shape. Any such improvements can be accommodated by blade element theory. Despite the fact that approach plans must be planned with such conceptual shifts. Only by estimating the so-called propeller-induced velocity, which changes the AOA seen by the blade components, can the BET produce an accurate depiction of the propeller. The airspeed within the propeller streamtube is higher than the surrounding air, which causes this effect. To explain the induced velocity inside the streamtube.

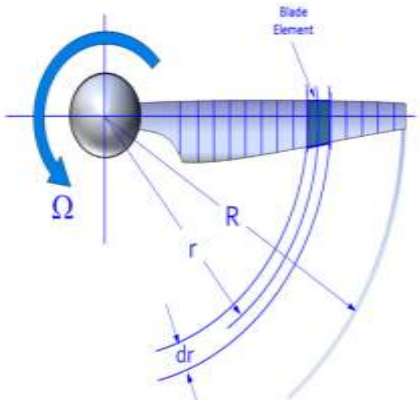

Fig-1: blade element formulation

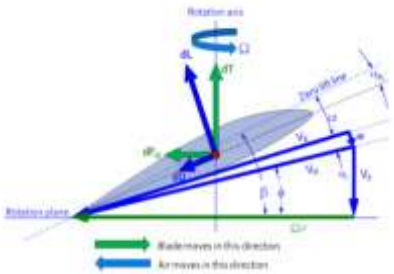

Fig-2: rotation of propeller & air moving direction

ADVANCE RATIO: J =V /n.D
PROPELLER EFFICIENCY: $\eta P = J. C_T/ C_P$
THRUST COEFFICIENT: $CT = T / \rho. n^2. D^4$
TORQUE COEFFICIENT: $CQ = Q / \rho.n^2 .D^5$
POWER COEFFICIENT: $CP = P / \rho. n^3 .D^5$

II. LITERATURE SURVEY

The computational techniques used in the present work for the measurement of thrust, power and torque for the ducted and unducted propellers using k-epsilon turbulence model. Using the thrust, power and torque measurements, we compare the basic theories involved with ducted and unducted propeller to the behaviour of various parameters like pressure, velocity contours been presented.Further, the thrust, torque and power characteristics has been studied for the development of ducted and unducted propeller.

A propeller can be thought of as a spinning wing that assembles airfoils into a single unit, similar to the cross-section of an airplane's wing. A simple propeller configuration consists of at least two blades connected by a central hub.

Earlier Stipa (1931) and Kort (1934) were the first to propose ducted propellers, and they are often used on vessels with high thrust requirements in the low speed range. The flow characteristics of the ducted propulsion system as a whole. The connection between the duct and the propeller is very intense.

The works of Abdel-Maksoud and Heinke (2002) and Krasilnikov et al. (2007) concluded, based on comprehensive RANSE computations, that the scale effects on the characteristics of ducted propulsion geometry (duct form and blade) affects propellers duct profile as well as loading conditions.

Propeller efficiency can be determined using a variety of methods, including experimental and numerical analysis. The propeller blade is tested in a wind tunnel for both static and

International Journal of Advances in Engineering and Management (IJAEM)
Volume 3, Issue 6 June 2021, pp: 1139-1147 www.ijaem.net ISSN: 2395-5252

advancing flow conditions in the experimental process. Numerical analysis, on the other hand, employs a three-dimensional approach. Simulation of computational fluid dynamics (CFD) using the Reynolds-average Navier–Stokes equation (RANS) equation. For propeller design and analysis, CFD methods have grown in importance and utility.

Over the last few decades, the production and use of unmanned aerial vehicles (UAVs) has exploded. As a result, it's critical to look into propeller performance to ensure that the design has resulted in a consistent UAV performance.

Benini conducted a study to compare the methods for determining propeller blade performance, including combined momentum-blade element theory and completely three-dimensional numerical RANS using CFD Fluent. The result demonstrates that the numerical approach used produces consistent results regardless of the advance ratio, with a maximum difference of 5% as compared to experimental results.

III. METHODOLOGY

PRELIMINARY DESIGN ANALYSIS:

In this paper, we have used NACA 24012airfoil for the designing of propeller blade. We have done some preliminary analysis of airfoil and its corresponding propeller blade using Qblade software. Fig-3 shows the profile of airfoil used in the propeller. The airfoil data taken from the online sources named AIRFOIL TOOLS.

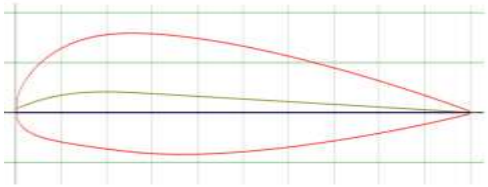

Fig-3: airfoil profile of NACA 24012

The aerodynamic performance curves for this airfoil at a velocity of 15m/s i.e. Reynolds number=27000 at 6.5 degree AOA which is usually this is airfoil section at 75% of propeller blade from hub. The propeller blade shown in figure 3.5 is created in Qblade inbuilt design environment using the above NACA 24012 airfoil through it, blade is divided in to 10 sections and the data of the sections are tabulated in Table-1. The cl, cd, cm vs 6.5 degree AOA of blade section at 75% of the blade. The plots are generated in Qblade airfoil analysis environment as shown in figures below.

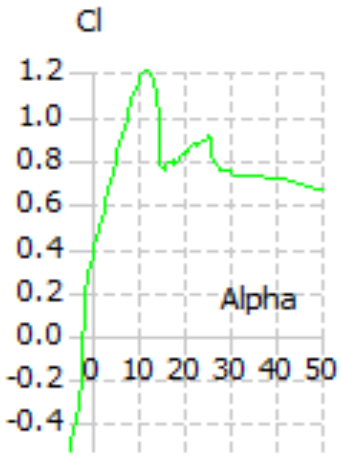

Fig-4: Cl vs AOA

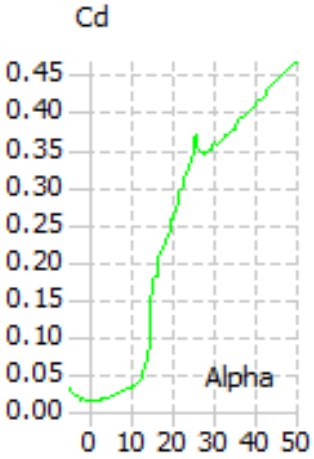

Fig-5: Cd vs AOA

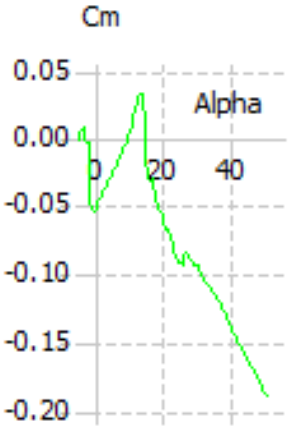

Fig-6: C_m vs AOA

International Journal of Advances in Engineering and Management (IJAEM)
Volume 3, Issue 6 June 2021, pp: 1139-1147 www.ijaem.net ISSN: 2395-5252

	Pos (mm)	Chord (mm)	Twist
1	0	10	-35
2	12.1	13	-25
3	24.2	17	-10
4	36.3	23	-3
5	48.4	27.5	1
6	60.5	29	3
7	72.6	28.5	5
8	84.7	26	6
9	96.8	22	7
10	108.9	16	8
11	121	8	8

Table-1: propeller blade span wise sections details

The blades is aligned with a maximum thickness location i.e. Thread at centreline maximum thickness. The blade has twist of 35 degrees at hub and 8 degrees twist at tip of the blade. Since the Qblade is a preliminary design tool it will design only blades leaving empty space at hub with diameter of hub between the hub portions of blades.

The resulted propeller blade with a hub radius of 10mm shown in fig-7.

The simulation performed using QLLT the nonlinear lifting line simulation. Further, the blade inputs are given such that blades rotated at 6000RPM is simulated at wind speed of 15m/s at 10% turbulence intensity with a ground effect, gravitational effect at a height 250m above sea-level illustrated in fig-8.

Fig-7: propeller design modelled in Qblade

The preliminary analysis results found to be that it has a thrust of around 4.1N and a torque of 0.08764 N-m

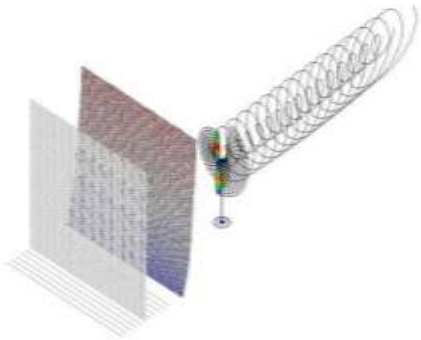

Fig-8: simulation of propeller in a wind turbulence model using Qblade

PROPELLER MODEL

As a result, the propeller is used as the reference configuration in this study since it is one of the most commonly used blades for UAVs. Analysis is performed on the ducted and unducted propeller with propeller diameter of 266.4mm at a velocity of 15m/s i.e. at a Reynolds number of 27000. Both the ducted propeller and unducted propeller modelled in CATIA as per the table-1 as shown in fig-11 and fig-10 respectively. Duct used in this paper is decelerating duct.

Fig-9: duct profile

Fig-10 unducted propeller modelled in CATIA

International Journal of Advances in Engineering and Management (IJAEM)
Volume 3, Issue 6 June 2021, pp: 1139-1147 www.ijaem.net ISSN: 2395-5252

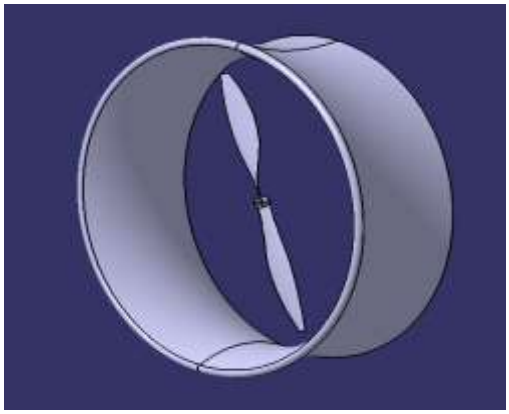

Fig-11: ducted propeller modelled in CATIA

The profile of the duct used is shown in the Fig-9:.with a leading edge lip diameter of 12mm.

NUMERICAL SETUP

Computational Domain around the propeller geometry has created using ANSYS DESIGN MODELER 19.1. CFD of the both ducted and unducted propeller is done by using sliding mesh approach using ANSYS fluent 19.1. The computational domain of both ducted and unducted propeller is shown in the fig-13 &12.

Inside the computational domain, the small cylinder over the propeller is used as rotating domain and the outer cylinder is stationary domain. In sliding mesh approach we define propeller as a stationery wall.The interface between the outer and inner cylindrical domain should be matched in terms of faces so that computation setup is done. Both the domains are defined as fluid and the propeller is defined as stationary wall.

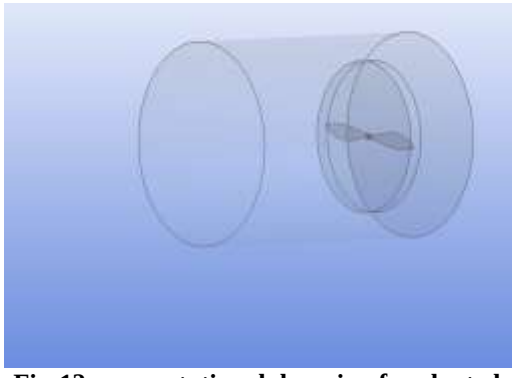

Fig-12: computational domain of unducted propeller

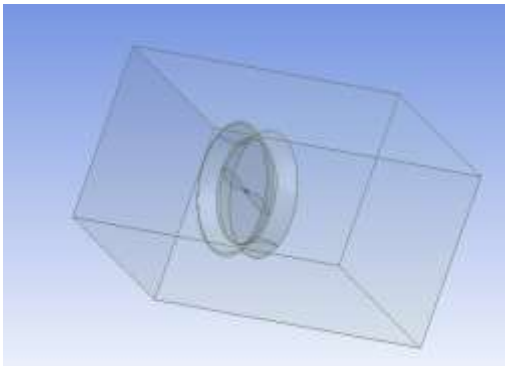

Fig-13: computational domain of ducted propeller

In ANSYS 19.1, a mesh tool was used to build the grid. The grid is important because it represents the geometry of interest in a unique way. The rate of convergence, the output obtained from the numerical analysis, and the computational time to run the analysis were all directly affected by the consistency of the computational grid.

The meshing details of the computational domains are shown the tables below. In both stationary and rotating domains, the grid is totally tetrahedral and unstructured. The decision is based on the rationale that unstructured tetrahedral grids can discretise complex geometries quickly and with minimal interactivity.

The mesh used here in this cfd is tetrahedron mesh with a minimum length of 29 mm with a normal angle of 18degrees ,and minimum curvature size of 0.29 mm. The mesh has a growth rate of 1.2 with a maximum sizing of 35mm and amximum proximity size of 0.29mm. The mesh element order is linear. The inflation use around the propeller with a maximum layers of 10 and its first layer thickness of 1mm normal to blade surface.

Sizing	
Use Adaptive Sizing	No
Growth Rate	Default (1.2)
Max Size	35.0 mm
Mesh Defeaturing	No
Capture Curvature	Yes
Curvature Min Size	Default (0.29 mm)
Curvature Normal Angle	Default (18.0°)
Capture Proximity	Yes
Proximity Min Size	Default (0.29 mm)
Num Cells Across Gap	Default (3)
Proximity Size Function Sources	Faces and Edges
Bounding Box Diagonal	795.44 mm
Average Surface Area	54448 mm²
Minimum Edge Length	0.47966 mm

Inflation	
Use Automatic Inflation	All Faces in Chosen Named Selection
Named Selection	propeller
Inflation Option	Smooth Transition
Transition Ratio	0.59
Maximum Layers	10
Growth Rate	1.2
Inflation Algorithm	Pre
View Advanced Options	No

International Journal of Advances in Engineering and Management (IJAEM)
Volume 3, Issue 6 June 2021, pp: 1139-1147 www.ijaem.net ISSN: 2395-5252

Object Name	Mesh
State	Solved
Display	
Display Style	Use Geometry Setting
Defaults	
Physics Preference	CFD
Solver Preference	Fluent
Element Order	Linear
Element Size	29.0 mm
Export Format	Standard
Export Preview Surface Mesh	No
Quality	
Check Mesh Quality	Yes, Errors
Target Skewness	Default (0.900000)
Smoothing	High
Mesh Metric	Orthogonal Quality
Min	5.8657e-002
Max	0.99671
Average	0.69171
Standard Deviation	0.15544

Table-2: Meshing details

The tetrahedon wireframe section is shown in the fig-16.the expontentially denser region init shows the rotating domain which has more cells i.e. lower mesh size compared to stationary domain as it needs more refined mesh to more accurary of propeller blade study .

Boundary conditions of CFD simulations were carried out with a rotational speed of 6000 RPM in the flow conditions, the free-stream velocity of 15m/s is defined on the inlet boundary, with a turbulence intensity of 10%.

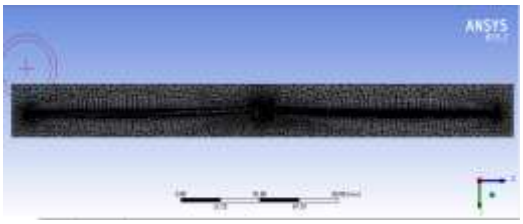

Fig-14: mesh of rotating domain

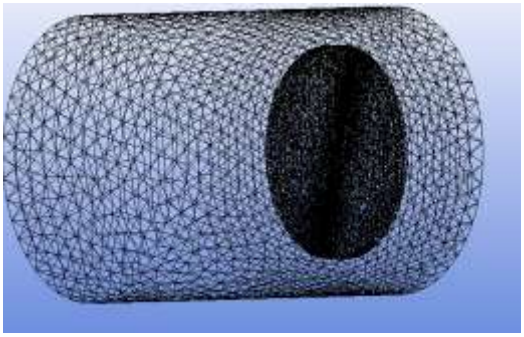

Fig-15: mesh grid in wireframe view of computational domain of unducted propeller.

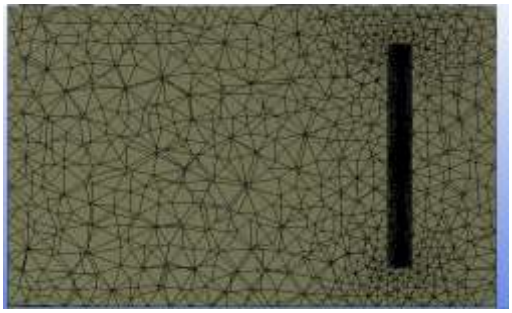

Fig-16: cut section view of computational domain of unducted propeller

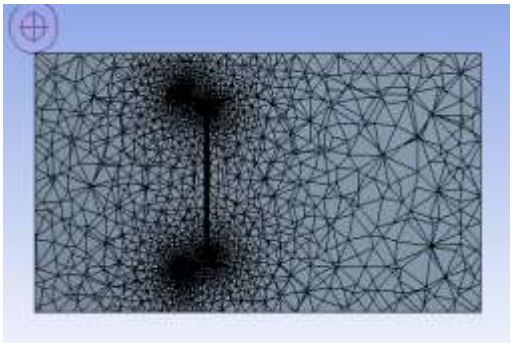

Fig-17: cut section view of computational domain of ducted propeller

Outflow boundary conditions were set at the flow exits downstream of the flow domain to set the turbulence strength based on the interactive conditions on the walls, a no-slip condition has been created. To integrate the rotational speed, the sliding mesh relation is assigned to the domain that encloses the propeller blade. SIMPLE method is applied for solving the solution.

Statistics	
Nodes	220162
Elements	710371

Fig-18: mesh nodes and elements

The method is particularly well suited to the study, which necessitates the interaction of stationary and rotating frames. Specific zones will have distinct rotational speeds assigned to them. A local frame transformation will be performed on the interface between the two regions allowing one zone's flow vector to be used by neighbouring zones. The propeller blade and hub walls were also designated as rotational, with zero velocity in relation to the adjacent cell zone. A Semi-Implicit Method for Pressure-Linked Equations is used to achieve the pressure–velocity coupling (SIMPLE).

International Journal of Advances in Engineering and Management (IJAEM)
Volume 3, Issue 6 June 2021, pp: 1139-1147 www.ijaem.net ISSN: 2395-5252

Momentum and pressure were calculated using the Second Order Upwind scheme. The gradients were calculated using the First Order Upwind for Turbulent Kinetic Energy and Turbulent Dissipation Rate, as well as the Least Square Cell-based Algorithm. For this, first-order algorithms generated accurate results.

The stationary region's inlet, outlet, and outer boundaries are far enough away from the propeller to prevent the complete production of the upstream and downstream flow from influencing the analysis' performance. The rotating domain is subdivided into a global stationary domain and a subdivided rotating field. The rotating domain is defined by a small cylindrical domain that completely encloses the propeller blades and hub. CFD simulations were run with a fixed rotational speed of 6000 RPM in the flow conditions. The free-stream velocity of 15m/s is defined on the inlet boundary, with a turbulence intensity of 10%. At the flow exits downstream of the flow domain, outflow boundary conditions were set. On the walls, a no-slip condition has been created. The sliding mesh reference is assigned to the domain that encloses the propeller blade in order to integrate the rotational speed. The inlet type is velocity inlet, outlet is pressure outlet and the walls are no slip stationary walls with a roughness of 0.5mm.

IV. RESULTS

To check the effect of the duct and the accuracy of the obtained data, the computational analysis results of ducted propellers were compared to unducted propeller data. The torque and thrust comparison is shown in the below table.

Propulsion Type	Thrust	Torque
Unducted propeller	3.478N	0.1896 N-m
Ducted propeller	4.12N	0.112 N-m

Table-3: thrust and torque

The velocity and pressure contours is shown in the below figures.

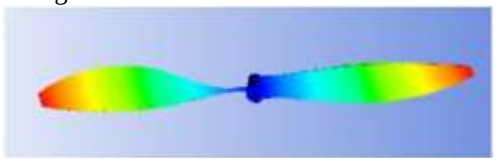

Fig-19: velocity contour over propeller

The propeller blade's pressure contour while running at an advance ratio of J is equal to 0.0093. The pressure at the back-side of the propeller is significantly higher than the pressure at the front-side of the propeller, as seen in the diagram. Thrust is generated when the pressure differential between the front and back sides of the propeller creates force in the forward direction.

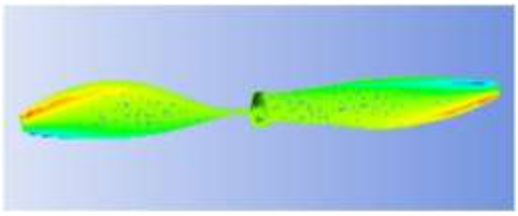

Fig-20: pressure contour over top surface of propeller

The comparative analysis of both pressure and velocity contours of both unducted and ducted propeller shows the p thrust produced by the ducted propeller is more than the unducted propeller at low flow free stream velocity conditions. Due to positive torque produced by the propellers in both the cases it is found that this model is optimally efficient at their own pace.Under same boundary conditions applied for the conventional and ducted propeller .It is found from the results that using the duct the overall thrust of the propulsive system is increased by 18.46%.

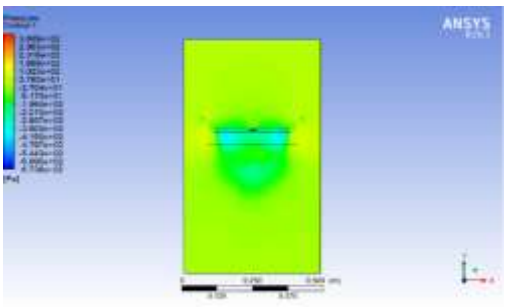

Fig-21: pressure contour of ducted propeller

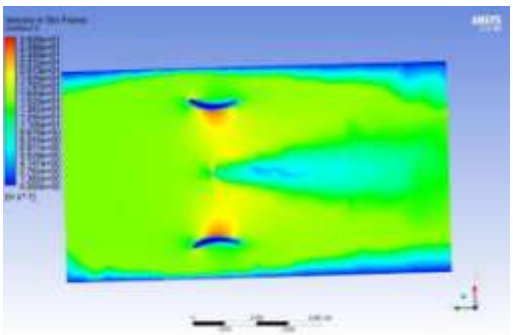

Fig-22: velocity contour of ducted propeller

International Journal of Advances in Engineering and Management (IJAEM)
Volume 3, Issue 6 June 2021, pp: 1139-1147 www.ijaem.net ISSN: 2395-5252

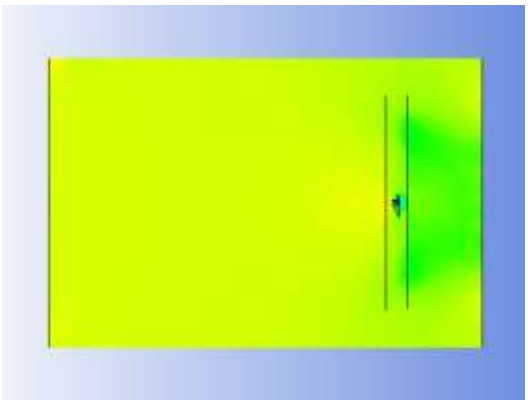

Fig-23: pressure contour of unducted propeller

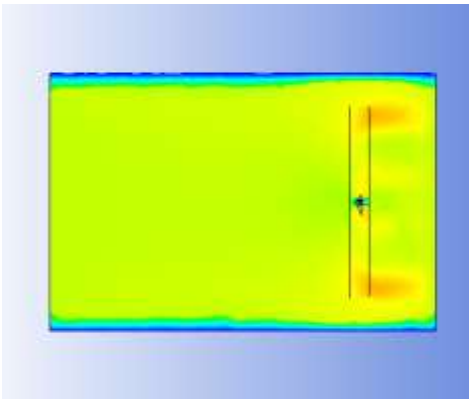

Fig-24: velocity contour of unducted propeller

V. DISCUSSION

The basic k-epsilon turbulence model is better suited to low Reynolds number aerospace applications. In addition, the model was able to predict the transformation model and improve the model's accuracy. At an advance ratio of J =0.0093, the pressure contour of the propeller blade is seen. The pressure at the back-side of the propeller is significantly higher than the pressure at the front-side of the propeller, as seen in the diagram. The pressure difference between the top and bottom surfaces of a propeller blade produces lift power, which allows the UAV to rise. The approach proposed in this study incorporates the rotational effect of the propeller blade by using a typical k-turbulence model and a Multiple Reference Frame model. The mesh-independent analysis looked at how the meshing number affected the entire domain. Overall, the results demonstrated a reliable ability to predict the efficiency of a small-scale propeller with a low Reynolds number and low speed. The amount of time it takes to make a decision on the final meshing is computed.

The thrust showed a slight under-prediction for a low advance ratio, while the power coefficient showed both an under-prediction and a slight under-prediction for a low advance ratio as compared to Qblade. Also under the same flow boundary conditions the thrust of the ducted propeller is found to be increased by 18.46% ascompared to the thrust produced by the conventional propeller.

VI. CONCLUSION

The objective of this study was to investigate and demonstrate the effectiveness of the propeller and unducted propeller. This current study provides opportunities to investigate various propeller blade configurations; reliable datasets for small-scale low-power applications can be collected through high fidelity method CFD ANSSY fluent 19.1. Using duct over a propeller increase the performance of propeller at low flow conditions which satisfies the requirements of additional thrust where it requires more at starting movement of UAV i.e. more acceleration or more thrust needed condition at low speeds. Significant parts of the blades cross sections work at stall conditions at low advance ratios that are much lower than the advance ratio at which the propeller's optimum efficiency is achieved. At low advance ratios, calculating the propeller's aerodynamic efficiency using two-dimensional non rotating airfoil data results in significant differences between the estimated and measured performance. Also the performance of the ducted propeller lowers with increase in higher velocity condition as compared to the unducted this is due limited intake mass flow for propeller. But at lower flow velocities the ducted propeller is found to be more efficient as compared to the unducted propeller.

To account for the rotational effect of the propeller blade, the approach proposed in this study employs a typical k-turbulence model and a sliding mesh Reference Frame model. Overall, the results demonstrated a reliable ability to predict the efficiency of a small-scale propeller with a low Reynolds number and low speed.

VII. FUTURE WORK

In future, when considering the potential reach of propellers, its worth considering the rate at which aircraft and engine production has progressed over the last six years, as this progress would not have been possible without the

intervention of war. The present work shows that small propellers at low Reynolds number, which is efficient at their pace. In future, because of the conquest of achieving high speed i.e. high Reynolds number flow, the propeller design R&D is further expanded and its fidelity is growing tremendous for UAV's and other high scale electric propellers aircraft in avoiding pollution. The propeller designer was well aware of these concurrent trends, and in order to satisfy them, we can accelerate this research and development further.

REFERENCES

[1]. Subhas, S. 2012. "CFD analysis of a propeller flow and cavitation." International Journal of Computer Applications 55(16) 26-33.

[2]. Anirban Bhattacharyya, V. K. 2016. "A CFD-based scaling approach for ducted propellers." ELSEVIER 116-130.

[3]. ANSYS, Inc. 2021. ANSYS Fluent User's Guide. http://users.abo.fi/rzevenho/ansys%20fluent%2018%20tutorial%20guide.pdf.

[4]. APC Slow Flyer 2021. https://www.apcprop.com/Articles.

[5]. Applications, International Journal of Computer. 2005. "Propeller Performance at Low Advance Ratio." JOURNAL OF AIRCRAFT 435-441.

[6]. Brandt, J.B., and M.S. Selig. 2013. "Propeller Performance data at low reynolds numbers." In Proceedings of the 49th AIAA Aerospace Sciences Meeting. grapevine, TX, USA: AIAA. 1-18.

[7]. Chang. 1998. Application of CFD to P4119 propeller. france: 22nd ITTC Propeller RANS/Panel Method Workshop.

[8]. Deters, R.W., G.K.A. Krishnan, and M.S Selig. 2014. "Reynolds number effects on the performance of small-scale propellers." AIAA Applied Aerodynamics Conference. , Atlanta, GA, USA: AIAA. 1-43.

[9]. ANSYS.INC, ANSYS. 2021. " ANSYS Fluent ." ANSYS Fluent User's Guide. http://users.abo.fi/rzevenho/ansys%20fluent%2018%20tutorial%20guide.pdf.

[10]. Morgado, J., M.Â.R. Silvestre, and J.C Páscoa. 2015. "Validation of new formulations for propeller Analysis." J. Propuls power 467-477.

[11]. Rajendran, Hairuniza Ahmed Kutty and Parvathy. 2017. 3D CFD Simulation and Experimental Validation of Small APC Slow Flyer Propeller Blade. School of Aerospace Engineering, Universiti Sains Malaysia, Penang 14300, Malaysia: MDPI.

[12]. S Subhas, V F Saji, S Ramakrishna and H N Das. 2017. "CFD Analysis of a Propeller Flow and Cavitation." International Journal of Computer Applications 22-33.

[13]. Wang, X., and K.S. Walter. 2012. Computational analysis of marine-propeller performance using transition-sensitive turbulence modelling. J. Fluids Eng.